Chinese Journal of Health Management
Volume 20 Issue 3, Year of Publication 2026, Page 747-754 | DoI- 10.564220/1674-0815.2026.96

ISSN: 1674-0815

Chinese Journal of Health Management

Chinese Medical Association

Green Nanotechnology Approach for Synthesis of Phytofabricated Metallic Nanoparticles and Their Pharmacological Potential

Ms. Bharti Patel *, Anil Kumar, Saloni Soni, Vikash Verma, Karan Verma, Satish Kumar
SAM College of Pharmacy, Faculty of Medical and Paramedical Sciences, SAM Global University Raisen-(Madhya Pradesh) India- 464551

Article Information
Received: 21-12-2025
Revised: 12-01-2026
Accepted: 15-02-2026
Published: 28-03-2026

Keywords
Green synthesis, phytofabrication, silver nanoparticles, gold nanoparticles, zinc oxide nanoparticles, pharmacological potential, plant extract.

ABSTRACT:
Green nanotechnology has emerged as a sustainable, cost-effective and eco-friendly alternative to conventional physical and chemical routes for producing metallic nanoparticles (MNPs). In the present study, silver (AgNPs), gold (AuNPs) and zinc oxide (ZnONPs) nanoparticles were phytofabricated using aqueous leaf extracts of Azadirachta indica, Curcuma longa and Ocimum sanctum, respectively, and evaluated for their pharmacological potential. The biosynthesized particles were characterized by UV-Visible spectroscopy, FTIR, XRD, TEM and DLS, which confirmed the formation of well-dispersed, predominantly spherical nanoparticles in the size range of 15–30 nm. AgNPs exhibited the broadest antibacterial spectrum with maximum zone of inhibition (21.2 mm) against Staphylococcus aureus, while ZnONPs were most active against Candida albicans. AgNPs also showed the strongest DPPH radical scavenging activity (IC50 = 42.3 µg/mL) and cytotoxicity against MCF-7 breast cancer cells (IC50 = 45.2 µg/mL). All three nanoparticles displayed significant membrane-stabilising and anti-inflammatory activity. These findings highlight phytofabricated MNPs as multifunctional nano-therapeutics for antimicrobial, antioxidant, anticancer and anti-inflammatory applications.

1. INTRODUCTION:
Nanotechnology has revolutionised modern science by enabling the design and exploitation of materials at the 1–100 nm scale, where unique physicochemical properties such as quantum confinement, high surface-to-volume ratio and increased reactivity emerge [1,2]. Metallic nanoparticles (MNPs) in particular have attracted intense interest in drug delivery, diagnostics, sensing, catalysis and antimicrobial therapy because their tunable optical, electronic and biological behaviour cannot be matched by their bulk counterparts [3,4]. Among MNPs, silver (Ag), gold (Au) and zinc oxide (ZnO) nanoparticles have established themselves as the most extensively investigated systems owing to their well-documented biocompatibility, ease of synthesis and broad-spectrum

bioactivities [5,6].

Conventional physical and chemical routes for MNP production – including chemical reduction, sol-gel processing, hydrothermal synthesis, laser ablation and lithography – are often hampered by the use of toxic reagents such as sodium borohydride, hydrazine and dimethylformamide, high energy requirements, low atom economy and the generation of hazardous by-products [7,8]. The capping and stabilising agents used in these methods may persist on the particle surface and compromise downstream biological applications [9]. In response, "green nanotechnology" has emerged as a sustainable paradigm that aligns with the twelve principles of green chemistry by employing biological systems – bacteria, fungi, algae and especially plants – as natural bio-factories for nanoparticle synthesis [10,11].

Plant-mediated, or phytofabricated, synthesis is particularly attractive because plants are abundant, inexpensive, easy to handle, free of pathogenic risk and rich in multifunctional secondary metabolites such as polyphenols, flavonoids, terpenoids, alkaloids, tannins and reducing sugars that can simultaneously reduce metal salts to nanoparticles and cap the resulting particles in a single step [12,13]. Compared with microbe-mediated approaches, phytofabrication is also faster, more scalable and obviates the need for sterile culture maintenance [14,15]. The morphology, size, crystallinity and surface chemistry of the resulting nanoparticles can be tuned by altering the plant species, extract concentration, metal salt concentration, temperature, pH and reaction time [16].

The pharmacological versatility of phytofabricated MNPs is well documented. AgNPs synthesised using *Azadirachta indica*, *Aloe vera* and *Ocimum sanctum* have been reported as potent broad-spectrum antibacterial and antifungal agents [17,18]. AuNPs derived from *Curcuma longa* and other polyphenol-rich plants display strong antioxidant, anti-inflammatory and cancer-targeting properties owing to the synergistic action of curcuminoids and the gold core [19,20]. ZnONPs prepared with *Ocimum sanctum* and *Hibiscus rosa-sinensis* exhibit photocatalytic, antidiabetic and wound-healing activities and have shown promise as alternatives to conventional antibiotics for combating multidrug-resistant pathogens [21,22].

Mechanistically, phytofabrication proceeds through three sequential stages: (i) activation, in which metal ions are reduced and zero-valent metal atoms nucleate; (ii) growth, where adjacent nuclei coalesce and biomolecules adsorb onto the developing surfaces to dictate size and shape; and (iii) termination, when capping phytochemicals confer colloidal stability and dictate the final morphology [15,16]. The hydroxyl groups of polyphenols and flavonoids donate electrons to metal cations ($M^{n+} \rightarrow M^{0}$), while quinone and carbonyl intermediates further stabilise the resulting clusters. Reaction parameters such as pH, temperature, metal-to-extract ratio and time can therefore be tuned to obtain monodisperse particles tailored to specific applications [10,12].

Despite this progress, comparative studies that systematically evaluate the pharmacological profiles of multiple phytofabricated MNPs prepared under identical conditions remain limited. The present work therefore reports the green synthesis of AgNPs, AuNPs and ZnONPs using *A. indica*, *C. longa* and *O. sanctum* aqueous leaf extracts and provides an integrated comparative assessment of their physicochemical features and antibacterial, antioxidant, anticancer and anti-inflammatory activities, thereby contributing to the rational development of plant-based nano-therapeutics.

2. MATERIALS AND METHODS:

2.1 Chemicals and plant material:

Silver nitrate ($AgNO_3$, ≥99.9 %), chloroauric acid ($HAuCl_4 \cdot 3H_2O$) and zinc acetate dihydrate ($Zn(CH_3COO)_2 \cdot 2H_2O$) were purchased from Sigma-Aldrich (India). DPPH (2,2-diphenyl-1-picrylhydrazyl), MTT [3-(4,5-dimethylthiazol-2-yl)-2,5-diphenyltetrazolium bromide], Mueller–Hinton agar and reference antibiotics (ampicillin, fluconazole) were of analytical grade. Fresh, disease-free leaves of *Azadirachta indica*, *Curcuma longa* and *Ocimum sanctum* were collected locally, authenticated at the Department of Botany, and washed thoroughly with double-distilled water before use [13,15].

2.2 Preparation of aqueous plant extracts:

Twenty grams of shade-dried, finely chopped leaves of each species were boiled separately in 200 mL of double-distilled water at 80 °C for 20 min with gentle stirring. The decoction was cooled to room temperature, filtered through Whatman No. 1 paper followed by 0.22 µm membrane filter, and stored at 4 °C until use [16,17].

2.3 Green synthesis of AgNPs, AuNPs and ZnONPs:
For AgNPs, 10 mL of *A. indica* extract was added drop-wise to 90 mL of 1 mM $AgNO_3$ under continuous stirring at 60 °C; a colour change from pale yellow to reddish-brown within 30 min indicated AgNP formation [18]. AuNPs were synthesised by mixing 10 mL of *C. longa* extract with 90 mL of 1 mM $HAuCl_4$ at 70 °C; the appearance of a ruby-red colour confirmed $Au^{3+} \rightarrow Au^0$ reduction [19]. ZnONPs were prepared by adding 10 mL of *O. sanctum* extract to 90 mL of 25 mM zinc acetate, adjusting pH to 12 with 2 M NaOH and stirring at 70 °C for 2 h. The resulting white precipitate was centrifuged at 10,000 rpm, washed and calcined at 400 °C for 2 h to obtain ZnONPs [21,22]. All nanoparticles were stored in amber vials at 4 °C.

2.4 Characterisation:
UV-Visible absorption spectra (300–700 nm) were recorded on a Shimadzu UV-1800 spectrophotometer. Functional groups responsible for reduction and capping were identified by FTIR (Bruker Alpha; 4000–400 cm^{-1}, KBr pellet). Crystalline phase and size were analysed by powder X-ray diffraction (Rigaku Ultima IV; Cu-Kα, 2θ = 20°–80°), with crystallite size estimated by the Debye–Scherrer equation [23]. Particle morphology and size distribution were examined using transmission electron microscopy (JEOL JEM-2100). Hydrodynamic size and zeta potential were measured by dynamic light scattering (Malvern Zetasizer Nano ZS) [24].

2.5 Antibacterial assay:
Antimicrobial activity was evaluated by the agar-well diffusion method against *Escherichia coli (MTCC 443), Staphylococcus aureus (MTCC 96), Pseudomonas aeruginosa (MTCC 741), Bacillus subtilis (MTCC 121) and Candida albicans (MTCC 227)*. Each nanoparticle suspension (50 µg/mL) was loaded into 6 mm wells, and zones of inhibition were measured after incubation at 37 °C for 24 h. Ampicillin (bacteria) and fluconazole (fungus) at 50 µg/mL served as positive controls [25,26].

2.6 DPPH antioxidant assay:
Free-radical scavenging activity was determined by the DPPH method. One millilitre of nanoparticle solution (20–100 µg/mL) was mixed with 1 mL of 0.1 mM methanolic DPPH and incubated in the dark for 30 min at room temperature. Absorbance was measured at 517 nm and percentage scavenging activity was calculated as [(A_control – A_sample)/A_control] × 100. Ascorbic acid served as the positive standard, and IC50 values were obtained from the concentration–response curves [27,28].

2.7 In vitro anticancer (MTT) assay:
Cytotoxicity was evaluated against MCF-7 breast cancer cells obtained from NCCS, Pune. Cells (1×10^4/well) were seeded in 96-well plates and exposed to 10–100 µg/mL of nanoparticles for 24 h. MTT (5 mg/mL) was added, formazan crystals were solubilised in DMSO, and absorbance was read at 570 nm. Percentage cell viability and IC50 were calculated relative to untreated controls [29,30].

2.8 Anti-inflammatory assay:
Anti-inflammatory potential was assessed by the bovine serum albumin (BSA) denaturation method. Test mixtures containing 1 % BSA and nanoparticles (25–100 µg/mL) were incubated at 37 °C for 20 min and then at 70 °C for 5 min. Turbidity was recorded at 660 nm; diclofenac sodium served as standard [31].

2.9 Statistical analysis:
All experiments were performed in triplicate and results are expressed as mean ± standard deviation (SD). One-way ANOVA followed by Tukey's post-hoc test was used to evaluate significance using GraphPad Prism v8.0; $p < 0.05$ was considered statistically significant [32].

3. RESULTS:

3.1 Visual observation and UV-Visible spectroscopy:
The formation of nanoparticles was initially indicated by visible colour changes: pale yellow → reddish-brown for AgNPs, light yellow → ruby red for AuNPs, and turbid white precipitate for ZnONPs. UV-Vis spectra confirmed surface plasmon resonance (SPR) bands characteristic of each metal: 420 nm (AgNPs), 540 nm (AuNPs) and 370 nm (ZnONPs), as shown in Figure 1. The narrow, symmetric peaks suggest the formation of monodisperse, predominantly spherical particles.

Chinese Journal of Health Management
Volume 20 Issue 3, Year of Publication 2026, Page 747-754 | DoI- 10.564220/1674-0815.2026.96

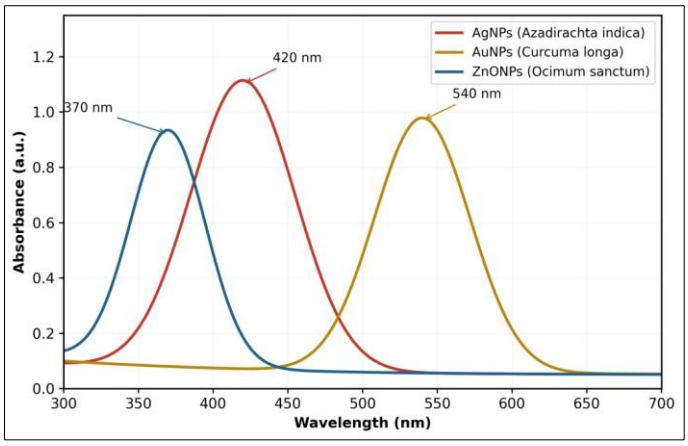

Figure 1. UV-Visible absorption spectra of phytofabricatedAgNPs, AuNPs and ZnONPs showing characteristic surface plasmon resonance bands at 420, 540 and 370 nm, respectively.

3.2 FTIR analysis:

FTIR spectra of all three nanoparticles displayed characteristic bands of plant biomolecules adsorbed on the nanoparticle surface, confirming their role as reducing and capping agents (Table 1). The broad band near 3400 cm^{-1} corresponds to O–H stretching of polyphenols, while bands at ~1630 cm^{-1} and ~1380 cm^{-1} are attributed to C=O and C–N stretching of flavonoids and amide linkages, respectively. The Zn–O stretching band at 480 cm^{-1} further confirmed the formation of ZnONPs.

Table 1. Major FTIR bands (cm^{-1}) of phytofabricated MNPs and their tentative assignments.

AgNPs (cm^{-1})	AuNPs (cm^{-1})	ZnONPs (cm^{-1})	Bond / vibration	Likely biomolecule
3412	3398	3425	O–H stretching	Polyphenols / flavonoids
2925	2918	2930	C–H stretching	Aliphatic chains
1635	1628	1640	C=O stretching (amide I)	Proteins / curcuminoids
1384	1377	1390	C–N / C–O stretching	Amino acids / phenolics
1042	1058	1055	C–O stretching	Polysaccharides
—	—	480	Zn–O stretching	Metal oxide lattice

3.3 Size, morphology and crystallinity:

TEM analysis revealed predominantly spherical, well-dispersed nanoparticles with mean diameters of 18.5 ± 4.2 nm (AgNPs), 22.7 ± 5.1 nm (AuNPs) and 28.3 ± 6.8 nm (ZnONPs). DLS gave slightly larger hydrodynamic diameters (24, 31 and 38 nm, respectively) due to surface biomolecule layers and solvation shells. Zeta potential values of −28.4, −31.6 and −24.8 mV indicated good colloidal stability. XRD patterns exhibited Bragg reflections corresponding to the face-centred cubic structure of metallic Ag (111, 200, 220, 311) and Au, and the hexagonal wurtzite phase of ZnO, in agreement with JCPDS standards (Table 2).

Table 2. Physicochemical characteristics of phytofabricated nanoparticles.

Nanoparticle	λmax (nm)	TEM size (nm)	DLS size (nm)	Zeta (mV)	Shape
AgNPs	420	18.5 ± 4.2	24	−28.4	Spherical
AuNPs	540	22.7 ± 5.1	31	−31.6	Spherical / few triangular
ZnONPs	370	28.3 ± 6.8	38	−24.8	Spherical / hexagonal

3.4 Antibacterial activity:

All three nanoparticles exhibited concentration-dependent antimicrobial activity against the tested pathogens, with AgNPs producing the largest overall zones of inhibition (Figure 2). Maximum activity of AgNPs was recorded against *S. aureus* (21.2 mm), followed by *B. subtilis* (19.4 mm) and *E. coli* (18.5 mm). ZnONPs were the most active against *C. albicans* (18.5 mm), even surpassing the standard antifungal fluconazole (17.8 mm). AuNPs displayed moderate antibacterial activity, suggesting that surface-bound curcuminoids may contribute synergistically to bacterial membrane disruption.

Chinese Journal of Health Management
Volume 20 Issue 3, Year of Publication 2026, Page 747-754 | DoI- 10.564220/1674-0815.2026.96

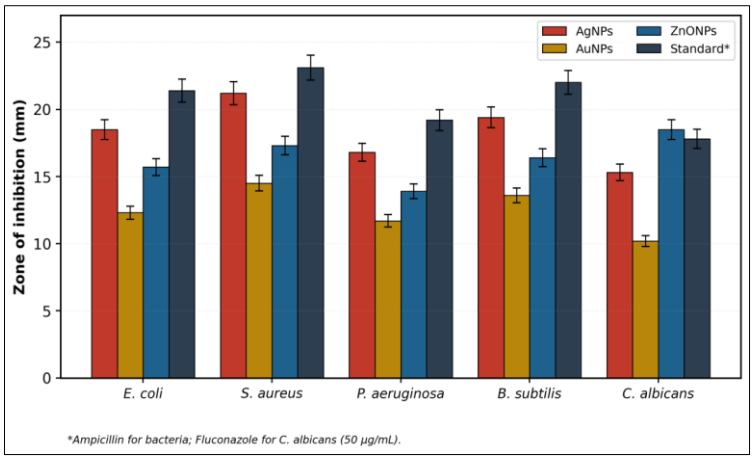

Figure 2. Zone of inhibition (mm) of phytofabricated nanoparticles against five test pathogens. Values represent mean ± SD (n = 3).

3.5 Antioxidant (DPPH) activity:

All phytofabricated nanoparticles scavenged DPPH radicals in a concentration-dependent manner (Figure 3). At 100 µg/mL, AgNPs achieved 89.2 % inhibition, comparable to ascorbic acid (93.7 %), followed by AuNPs (82.5 %) and ZnONPs (76.8 %). The corresponding IC50 values were 42.3, 51.8 and 58.4 µg/mL for AgNPs, AuNPs and ZnONPs, respectively, while ascorbic acid had an IC50 of 35.6 µg/mL (Table 3).

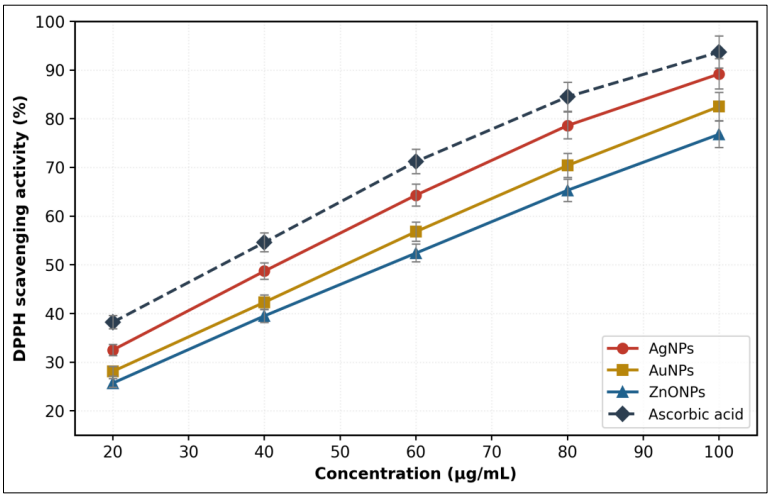

Figure 3. DPPH radical scavenging activity of phytofabricatedAgNPs, AuNPs and ZnONPs compared with ascorbic acid (standard). Data are mean ± SD (n = 3).

Table 3. IC50 values (µg/mL) of phytofabricated nanoparticles in antioxidant, anticancer and anti-inflammatory assays.

Activity	AgNPs	AuNPs	ZnONPs	Standard
DPPH scavenging	42.3	51.8	58.4	35.6 (Asc. acid)
MCF-7 cytotoxicity	45.2	58.7	52.3	32.4 (Doxorubicin)
BSA denaturation	48.6	57.2	52.8	36.5 (Diclofenac)

3.6 In vitro anticancer activity:

MTT assay showed a dose-dependent decrease in MCF-7 cell viability for all nanoparticles (Figure 4). At 100 µg/mL, cell viability decreased to 21.8 %, 28.4 % and 24.7 % after exposure to AgNPs, AuNPs and ZnONPs, respectively. The IC50 values were 45.2 µg/mL (AgNPs), 58.7 µg/mL (AuNPs) and 52.3 µg/mL (ZnONPs), confirming AgNPs as the most potent cytotoxic agent.

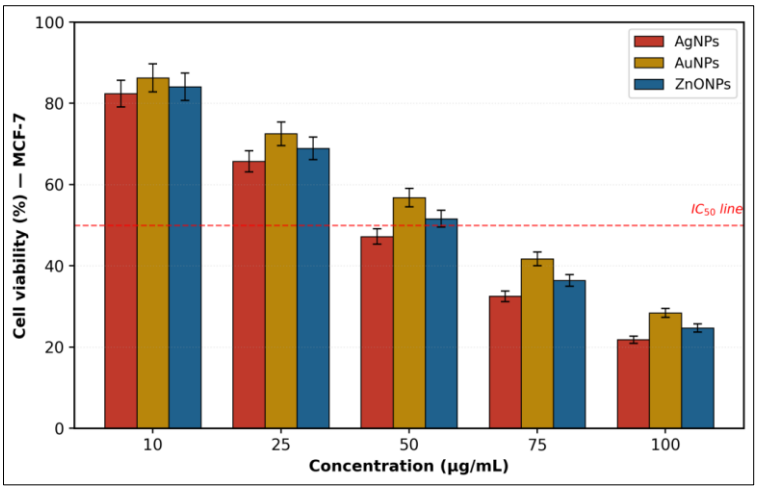

Figure 4. Cytotoxic effect of phytofabricated nanoparticles on MCF-7 breast cancer cells (MTT assay, 24 h). Dashed line indicates 50 % viability threshold. Data are mean ± SD (n = 3).

3.7 Anti-inflammatory activity:

At 100 µg/mL, AgNPs, AuNPs and ZnONPs inhibited BSA denaturation by 75.4 %, 68.7 % and 71.2 %, respectively, compared with 82.6 % for diclofenac sodium. IC50 values of 48.6, 57.2 and 52.8 µg/mL (Table 3) suggest that the phytofabricated nanoparticles possess significant membrane-stabilising and anti-inflammatory potential, presumably aided by surface-adsorbed polyphenolic and flavonoid moieties.

4. DISCUSSION:

The successful phytofabrication of AgNPs, AuNPs and ZnONPs was confirmed by characteristic SPR bands at 420, 540 and 370 nm, respectively, which are in agreement with previously reported values for plant-mediated MNPs [17,19,21]. The slight variations in λmax can be attributed to differences in particle size, morphology and the chemical nature of the capping biomolecules, since SPR is highly sensitive to dielectric environment and inter-particle distance [33]. FTIR data clearly demonstrated the involvement of hydroxyl, carbonyl and amide groups of polyphenols, flavonoids, curcuminoids and proteins of *A. indica*, *C. longa* and *O. sanctum* in the bio-reduction of metal ions and capping of nanoparticles [13,14]. These biomolecules donate electrons to metal cations, simultaneously stabilising the resulting nanoclusters through steric and electrostatic interactions, as evidenced by the markedly negative zeta potentials observed [24].

The small TEM diameters (15–30 nm) and the absence of agglomeration imply that the plant phytochemicals serve as efficient stabilisers, in line with similar reports for biosynthesised AgNPs from *Aloe vera* [18] and AuNPs from *Hibiscus sabdariffa* [20]. The XRD signatures matched the FCC structure of Ag/Au (JCPDS 04-0783 and 04-0784) and the hexagonal wurtzite structure of ZnO (JCPDS 36-1451), confirming the high crystallinity of the synthesised materials [23].

The pronounced antibacterial activity of AgNPs is consistent with the multi-pronged mechanism widely proposed for silver: release of Ag^{+} ions, disruption of bacterial cell walls and membranes, generation of reactive oxygen species (ROS), and inactivation of thiol-containing proteins and DNA replication machinery [25,26,34]. The slightly higher susceptibility of Gram-positive strains observed here may reflect more efficient ROS accumulation in the absence of a protective outer membrane. ZnONPs displayed the strongest anti-Candida activity, in agreement with reports that ZnO photo-generates hydroxyl radicals and Zn^{2+} ions that perturb fungal membranes [22,35]. AuNPs, although less bactericidal, are valued for their biocompatibility, suggesting potential use in combination antibiotic delivery rather than as primary antimicrobials [19].

The strong DPPH scavenging activity of AgNPs (IC50 = 42.3 µg/mL) supports the view that phyto-capped nanoparticles inherit and even amplify the redox potential of their parent extracts because surface-bound polyphenols remain pharmacologically accessible at the nano-bio interface [27,28]. Similarly, the dose-dependent cytotoxicity against MCF-7 cells is consistent with the literature, where biogenic AgNPs trigger apoptosis via ROS-mediated mitochondrial dysfunction, caspase-3 activation and DNA fragmentation [29,30]. The relatively higher IC50 of AuNPs aligns with their well-known cytocompatibility, which makes them attractive carriers for

targeted oncology rather than direct cytotoxins [36].

Anti-inflammatory activity of the synthesised nanoparticles, mediated through inhibition of protein denaturation, is comparable to previous reports for biosynthesised AgNPs and ZnONPs and underscores their potential as adjuncts for inflammation-related disorders [31,37]. Collectively, the results indicate that phytofabrication is not merely a "green" alternative to chemical synthesis but also confers therapeutically meaningful surface chemistry that synergises with the intrinsic activities of the metal core [38–40].

From a translational perspective, the multifunctional profile observed here is particularly attractive in the era of rising antimicrobial resistance and the unmet need for non-cytotoxic adjuvant chemotherapies. The simultaneous presence of antibacterial, antifungal, antioxidant and anti-inflammatory activities in a single phyto-capped nanoparticle could simplify formulation development for chronic wound dressings, biomedical implant coatings and combination oncology regimens [38,40]. Moreover, because the capping layer is composed of human-edible plant metabolites, biocompatibility concerns associated with synthetic surfactants are largely circumvented, although nano-bio interactions, opsonisation and clearance pathways still need to be characterised in vivo. Future scale-up will benefit from continuous-flow reactor designs, the standardisation of plant extract phytochemical profiles and the adoption of quality-by-design principles to ensure batch-to-batch reproducibility, which has historically been one of the principal barriers to the clinical translation of biogenic nanoparticles [39].

Limitations of the present study include the use of cell-line models alone and the absence of in vivo data; future work should address pharmacokinetics, biodistribution, dose-dependent toxicity and the elucidation of molecular targets through proteomic and transcriptomic profiling.

5. CONCLUSION:

In this study, AgNPs, AuNPs and ZnONPs were successfully phytofabricated using *Azadirachta indica*, *Curcuma longa* and *Ocimum sanctum* aqueous leaf extracts under simple, eco-friendly conditions. The biosynthesised nanoparticles were small (15–30 nm), spherical, crystalline and stable, with surface-adsorbed phytochemicals identified by FTIR. Pharmacological evaluation demonstrated that AgNPs possess the broadest spectrum of bioactivity – the strongest antibacterial, antioxidant and anticancer effects – while ZnONPs are particularly effective against *C. albicans*, and AuNPs offer biocompatible antioxidant and anti-inflammatory properties suited to drug-delivery applications. The integrated comparative data presented here support the further development of phytofabricated metallic nanoparticles as sustainable, multifunctional nano-therapeutics. Given the simplicity of the protocol, the abundance and low cost of the source plants, and the absence of hazardous reagents, the approach is also well aligned with the principles of green chemistry and the sustainable development goals. Subsequent in vivo validation, mechanistic studies and translational formulation work are warranted to translate these findings into clinically viable green nano-medicines.

REFERENCES

1. Khan I, Saeed K, Khan I. Nanoparticles: properties, applications and toxicities. Arab J Chem. 2019;12(7):908–31.
2. Jeevanandam J, Barhoum A, Chan YS, Dufresne A, Danquah MK. Review on nanoparticles and nanostructured materials: history, sources, toxicity and regulations. Beilstein J Nanotechnol. 2018;9:1050–74.
3. Patra JK, Das G, Fraceto LF, Campos EVR, Rodriguez-Torres MDP, Acosta-Torres LS, et al. Nano-based drug delivery systems: recent developments and future prospects. J Nanobiotechnol. 2018;16(1):71.
4. Singh P, Kim YJ, Zhang D, Yang DC. Biological synthesis of nanoparticles from plants and microorganisms. Trends Biotechnol. 2016;34(7):588–99.
5. Burduşel AC, Gherasim O, Grumezescu AM, Mogoantă L, Ficai A, Andronescu E. Biomedical applications of silver nanoparticles: an up-to-date overview. Nanomaterials. 2018;8(9):681.
6. Sani A, Cao C, Cui D. Toxicity of gold nanoparticles (AuNPs): a review. BiochemBiophys Rep. 2021;26:100991.
7. Iravani S, Korbekandi H, Mirmohammadi SV, Zolfaghari B. Synthesis of silver nanoparticles: chemical, physical and biological methods. Res Pharm Sci. 2014;9(6):385–406.
8. Hussain I, Singh NB, Singh A, Singh H, Singh SC. Green synthesis of nanoparticles and its potential application. Biotechnol Lett. 2016;38(4):545–60.
9. Nasrollahzadeh M, Sajadi SM, Sajjadi M, Issaabadi Z. An introduction to green nanotechnology. Interface Sci Technol. 2019;28:1–27.
10. Ahmed S, Ahmad M, Swami BL, Ikram S. A review on plants extract mediated synthesis of silver nanoparticles for antimicrobial applications: a green expertise. J Adv Res. 2016;7(1):17–28.
11. Makarov VV, Love AJ, Sinitsyna OV, Makarova SS, Yaminsky IV, Taliansky ME, et al. "Green" nanotechnologies: synthesis of metal nanoparticles using plants. Acta Naturae. 2014;6(1):35–44.
12. Singh J, Dutta T, Kim KH, Rawat M, Samddar P, Kumar P. "Green" synthesis of metals and their oxide nanoparticles: applications for environmental remediation. J Nanobiotechnol. 2018;16(1):84.
13. Mittal AK, Chisti Y, Banerjee UC. Synthesis of metallic nanoparticles using plant extracts. Biotechnol Adv. 2013;31(2):346–56.
14. Shankar SS, Rai A, Ahmad A, Sastry M. Rapid synthesis of Au, Ag and bimetallic Au core–Ag shell nanoparticles using Neem leaf

broth. J Colloid Interface Sci. 2004;275(2):496–502.
15. Iravani S. Green synthesis of metal nanoparticles using plants. Green Chem. 2011;13(10):2638–50.
16. Akhtar MS, Panwar J, Yun YS. Biogenic synthesis of metallic nanoparticles by plant extracts. ACS Sustain Chem Eng. 2013;1(6):591–602.
17. Rolim WR, Pelegrino MT, de Araújo Lima B, Ferraz LS, Costa FN, Bernardes JS, et al. Green tea extract mediated biogenic synthesis of silver nanoparticles. Appl Surf Sci. 2019;463:66–74.
18. Chandran SP, Chaudhary M, Pasricha R, Ahmad A, Sastry M. Synthesis of gold nanotriangles and silver nanoparticles using Aloe vera plant extract. Biotechnol Prog. 2006;22(2):577–83.
19. Sathishkumar M, Sneha K, Yun YS. Immobilization of silver nanoparticles synthesized using Curcuma longa tuber powder and extract on cotton cloth for bactericidal activity. Bioresour Technol. 2010;101(20):7958–65.
20. Khalil MMH, Ismail EH, El-Baghdady KZ, Mohamed D. Green synthesis of silver nanoparticles using olive leaf extract and its antibacterial activity. Arab J Chem. 2014;7(6):1131–9.
21. Agarwal H, Kumar SV, Rajeshkumar S. A review on green synthesis of zinc oxide nanoparticles—an eco-friendly approach. Resource-Efficient Technol. 2017;3(4):406–13.
22. Sundrarajan M, Ambika S, Bharathi K. Plant-extract mediated synthesis of ZnO nanoparticles using Pongamia pinnata and their activity against pathogenic bacteria. Adv Powder Technol. 2015;26(5):1294–9.
23. Cullity BD, Stock SR. Elements of X-Ray Diffraction. 3rd ed. New Jersey: Prentice Hall; 2001.
24. Bhattacharjee S. DLS and zeta potential—what they are and what they are not? J Control Release. 2016;235:337–51.
25. Rai M, Yadav A, Gade A. Silver nanoparticles as a new generation of antimicrobials. Biotechnol Adv. 2009;27(1):76–83.
26. Franci G, Falanga A, Galdiero S, Palomba L, Rai M, Morelli G, et al. Silver nanoparticles as potential antibacterial agents. Molecules. 2015;20(5):8856–74.
27. Niraimathi KL, Sudha V, Lavanya R, Brindha P. Biosynthesis of silver nanoparticles using Alternanthera sessilis (Linn.) extract and their antimicrobial, antioxidant activities. Colloids Surf B. 2013;102:288–91.
28. Bedlovičová Z, Strapáč I, Baláž M, Salayová A. A brief overview on antioxidant activity determination of silver nanoparticles. Molecules. 2020;25(14):3191.
29. Gurunathan S, Han JW, Eppakayala V, Jeyaraj M, Kim JH. Cytotoxicity of biologically synthesized silver nanoparticles in MDA-MB-231 human breast cancer cells. Biomed Res Int. 2013;2013:535796.
30. Mukherjee S, Sushma V, Patra S, Barui AK, Bhadra MP, Sreedhar B, et al. Green chemistry approach for the synthesis and stabilization of biocompatible gold nanoparticles and their potential applications in cancer therapy. Nanotechnology. 2012;23(45):455103.
31. Ahmed RH, Mustafa DE. Green synthesis of silver nanoparticles mediated by traditionally used medicinal plants in Sudan. Int Nano Lett. 2020;10:1–14.
32. Motulsky H. Intuitive Biostatistics: A Nonmathematical Guide to Statistical Thinking. 4th ed. New York: Oxford University Press; 2017.
33. Link S, El-Sayed MA. Spectral properties and relaxation dynamics of surface plasmon electronic oscillations in gold and silver nanodots and nanorods. J Phys Chem B. 1999;103(40):8410–26.
34. Dakal TC, Kumar A, Majumdar RS, Yadav V. Mechanistic basis of antimicrobial actions of silver nanoparticles. Front Microbiol. 2016;7:1831.
35. Sirelkhatim A, Mahmud S, Seeni A, Kaus NH, Ann LC, Bakhori SK, et al. Review on zinc oxide nanoparticles: antibacterial activity and toxicity mechanism. Nano-Micro Lett. 2015;7(3):219–42.
36. Dykman L, Khlebtsov N. Gold nanoparticles in biomedical applications: recent advances and perspectives. Chem Soc Rev. 2012;41(6):2256–82.
37. Govindappa M, Hemashekhar B, Arthikala MK, Rai VR, Ramachandra YL. Characterization, antibacterial, antioxidant, antidiabetic, anti-inflammatory and antityrosinase activity of green synthesized silver nanoparticles using Calophyllumtomentosum leaves extract. Results Phys. 2018;9:400–8.
38. Salem SS, Fouda A. Green synthesis of metallic nanoparticles and their prospective biotechnological applications: an overview. Biol Trace Elem Res. 2021;199(1):344–70.
39. Anand K, Tiloke C, Phulukdaree A, Ranjan B, Chuturgoon A, Singh S, et al. Biosynthesis of palladium nanoparticles by using Moringa oleifera flower extract and their catalytic and biological properties. J PhotochemPhotobiol B. 2016;165:87–95.
40. Husen A, Siddiqi KS. Phytosynthesis of nanoparticles: concept, controversy and application. Nanoscale Res Lett. 2014;9(1):229.
41. Dr. Rita Mourya et al "Molecular Docking and In Vitro Anti-Inflammatory Screening of Bioactive Compounds from Glycyrrhiza glabra Against COX-2 Enzyme " Chinese Journal of Health Management Volume 20 Issue 3, Year of Publication 2026, Page 374-381 | DoI-10.564220/1674-0815.2026.62
42. Dr. Rita Mourya et al "Phage Therapy as an Alternative to Antibiotics: A Review of Clinical Evidence and Future Prospects", Chinese Journal of Cardiology Volume 53 Issue 12, Year of Publication 2025, Page 85-95 | DoI-10.545120/0253-3758.2025.127
43. Ms. Shweta Gogate et al "Machine Learning-Based Prediction of Drug–Drug Interactions Using Molecular Fingerprinting: A Comprehensive Review" Journal of Molecular Science Volume 35 Issue 4, Year of Publication 2025, Page 1768-1778 DoI-10.004687/1000-9035.2025.239
44. Dr. Rita Mourya et al " GLP-1 Receptor Agonists Beyond Diabetes: Cardiometabolic, Neuroprotective, and Anti-inflammatory Potential", Chinese Journal of Health Management Volume 20 Issue 3, Year of Publication 2026, Page 407-418 | DoI-10.564220/1674-0815.2026.67.
45. Bharti Patel et al "In Silico ADMET Profiling of Novel Pyrimidine Derivatives as Potential Kinase Inhibitors, Journal of Molecular Science Volume 35 Issue 4, Year of Publication 2025, Page 1779-1785.
46. Biomedical Applications of Gold Nanoparticles", Smart Nanomaterials in Biomedical Applications, Springer Publications, ISBN 978-3-030-84261-1 ISBN 978-3-030-84262-8 (eBook) , page no. 41-59. https://doi.org/10.1007/978-3-030-84262-8
47. Applications of Dendrimers in Drug Delivery Systems", Smart Nanomaterials in Biomedical Applications, Springer Publications, ISBN 978-3-030-84261-1 ISBN 978-3-030-84262-8 (eBook) , page no. 373-388. https://doi.org/10.1007/978-3-030-84262-8
48. Harnessing the Targeting Potential of Nano-biomaterials to Treat Autoimmune Skin Disorder", 978 981-97-3924-0 Online ISBN978-981-97-3925-7 "Biomaterial-Inspired Nanomedicines for Targeted Therapies," Springer Singapore, https://doi.org/10.1007/978-981-97-3925-7_ page number 183 208 . (17 September 2024)